Biochemical and Biophysical Research Communications 466 (2015) 418–425

Contents lists available at ScienceDirect

Biochemical and Biophysical Research Communications

journal homepage: www.elsevier.com/locate/ybbrc

# Binding of dihydroxynaphthyl aryl ketones to tubulin colchicine site inhibits microtubule assembly

Eunices Gutierrez [a], Julio Benites [a, b], Jaime A. Valderrama [a, b, c], Pedro Buc Calderon [b, d], Julien Verrax [d], Esteban Nova [e], Felipe Villanelo [e], Daniel Maturana [e], Cristian Escobar [e], Rosalba Lagos [e], Octavio Monasterio [e, *]

[a] Facultad de Ciencias de la Salud, Universidad Arturo Prat, Iquique, Chile
[b] Instituto de EtnoFarmacologia (IDE), Universidad Arturo Prat, Iquique, Chile
[c] Facultad de Química, Pontificia Universidad Católica de Chile, Santiago, Chile
[d] Toxicology and Cancer Biology Research Group, Louvain Drug Research Institute, Université Catholique de Louvain, Brussels, Belgium
[e] Departamento de Biología, Facultad de Ciencias, Universidad de Chile, Santiago, Chile

ARTICLE INFO

*Article history:*
Received 27 August 2015
Accepted 8 September 2015
Available online 11 September 2015

*Keywords:*
Microtubules
Photo acylation
Dihydroxynaphthyl aryl ketones
Thermophoresis
Colchicine
Bioinformatics

ABSTRACT

Dihydroxynaphthyl aryl ketones **1**–**5** have been evaluated for their abilities to inhibit microtubule assembly and the binding to tubulin. Compounds **3**, **4** and **5** displayed competitive inhibition against colchicine binding, and docking analysis showed that they bind to the tubulin colchicine-binding pocket inducing sheets instead of microtubules. Remarkable differences in biological activity observed among the assayed compounds seem to be related to the structure and position of the aryl substituent bonded to the carbonyl group. Compounds **2**, **3** and **4**, which contain a heterocyclic ring, presented higher affinity for tubulin compared to the carbocyclic analogue **5**. Compound **4** showed the best affinity of the series, with an $IC_{50}$ value of 2.1 μM for microtubule polymerization inhibition and a tubulin dissociation constant of 1.0 ± 0.2 μM, as determined by thermophoresis. Compound **4** was more efficacious in disrupting microtubule assembly in vitro than compound **5** although it contains the trimethoxyphenyl ring present in colchicine. Hydrogen bonds with Asn101 of α-tubulin seem to be responsible for the higher affinity of compound **4** respects to the others.



## 1. Introduction

Microtubules are non-covalent polymers composed of α- and β-tubulin heterodimers that are assembled into a filamentous tube-shaped helicoidal structure [1]. Polymerization occurs through a dynamic process called dynamic instability, which depends on polymer structure and GTP hydrolysis [2]. The primary function of microtubules is to provide support for dynamic cellular processes, such as mitosis, and to maintain the shape of the cell. Microtubules are typically found in all eukaryotic cells and are a component of the cytoskeleton, cilia and flagella. Microtubules play an important role in cytoplasmic movements within the cell, and they form the spindle fibers that bind to the centromere and separate the chromosomes during mitosis. The important role of microtubules in cell division makes them a desirable target for the development of chemotherapeutic agents directed against rapidly dividing cancer cells [3]. Therefore, tubulin represents a promising drug target to inhibit cell proliferation [4]. Several antimitotic agents that are currently in clinical use as chemotherapies, including vincristine, vinblastine [5] and epothilones [6], exert their action by interrupting the dynamic instability of microtubules by inhibiting either tubulin polymerization or depolymerization through the stabilization of microtubules [7,8].

Among the drugs that modify the cytoskeleton, colchicine depolymerizes microtubules at μM concentrations [9,10], and it perturbs microtubule dynamics in the nM concentration range [11]. The structure of the tubulin binding sites of colchicine and podophyllotoxin were resolved by X-ray diffraction from their respective

*Nomenclature and abbreviations:* APS, ammonium persulfate; DMSO, dimethyl sufoxide; dNAKs, dihydroxynaphthyl aryl ketones; $E^{mM}$, extinction coefficient millimolar; ITP, inhibition tubulin polymerization; MTT, 3-(4,5-dimethylthiazol-2-yl)-2,5-diphenyltatrazolium bromide; NT-647, fluorescence probe; SDS, sodium dodecyl sulfate; TEMED, tetramethylendiamine.

* Corresponding author. Las Palmeras 3425, Santiago, CP 7800003, Chile.
*E-mail address:* monaster@uchile.cl (O. Monasterio).

http://dx.doi.org/10.1016/j.bbrc.2015.09.041
0006-291X/

crystal complexes [12]. However, these drugs have serious drawbacks that limit their applicability for the treatment of cancer due to the appearance of various side effects and their associated toxicity [13]. Thus, an intensive search is ongoing for compounds with similar activity, including natural and synthetic compounds that bind tubulin in the colchicine site [14]. In general, these families of compounds have 2 non-coplanar aromatic rings that are linked by a bridge of between 0 and 4 carbon atoms. In many cases, one of the rings is a trimethoxyphenyl derivative [15,16]. Although many synthetic tubulin inhibitors have been synthesized in recent years, there is still a need to identify novel molecules that target microtubules. Ideally, these compounds would have relatively simple structures and would be easy to prepare in a cost-effective manner.

Previously, we reported a flexible and inexpensive procedure to prepare dihydroxynaphthyl aryl ketones (dNAKs) [17]. This procedure was successfully extended to the preparation of a broad variety of diarylketones [18]. Considering the facile, inexpensive and eco-friendly access to dNAKs and the similarity of its structures to potent inhibitors of tubulin polymerization such as colchicine [9–11] and naphthylphenstatins [19], dNAKs **1**–**5** (Fig. 1) were selected for evaluation as tubulin polymerization inhibitors. The binding of dNAKs to tubulin colchicine site will be described at molecular level.

## 2. Materials and methods

### 2.1. Chemicals

Sephadex G-25, DEAE–Sephadex A-50, TEMED, sodium dodecyl sulfate, EGTA, GTP, ammonium persulfate, dimethyl sulfoxide and colchicine were purchased from Sigma–Aldrich Chem. Co. (St. Louis, MO, USA). Comassie R250, magnesium chloride, potassium chloride, disodium phosphate and sucrose were purchased from Merck (Darmstadt, Germany). Sodium monophosphate was obtained from Scharlau Chemie S.A. (Barcelona, Spain). Sephacryl S-300 was purchased from GE Healthcare Bio-Sciences AB (Rapsgatan, Uppsala, Sweden). Bisacrylamide was obtained from MP Biomedical, Inc. (Strasbourg, France). The protease inhibitors were purchased from CALBIOCHEM (Billerica, MA, USA), and the membrane dialysis materials were obtained from Spectrum labs (Ontario, Canada).

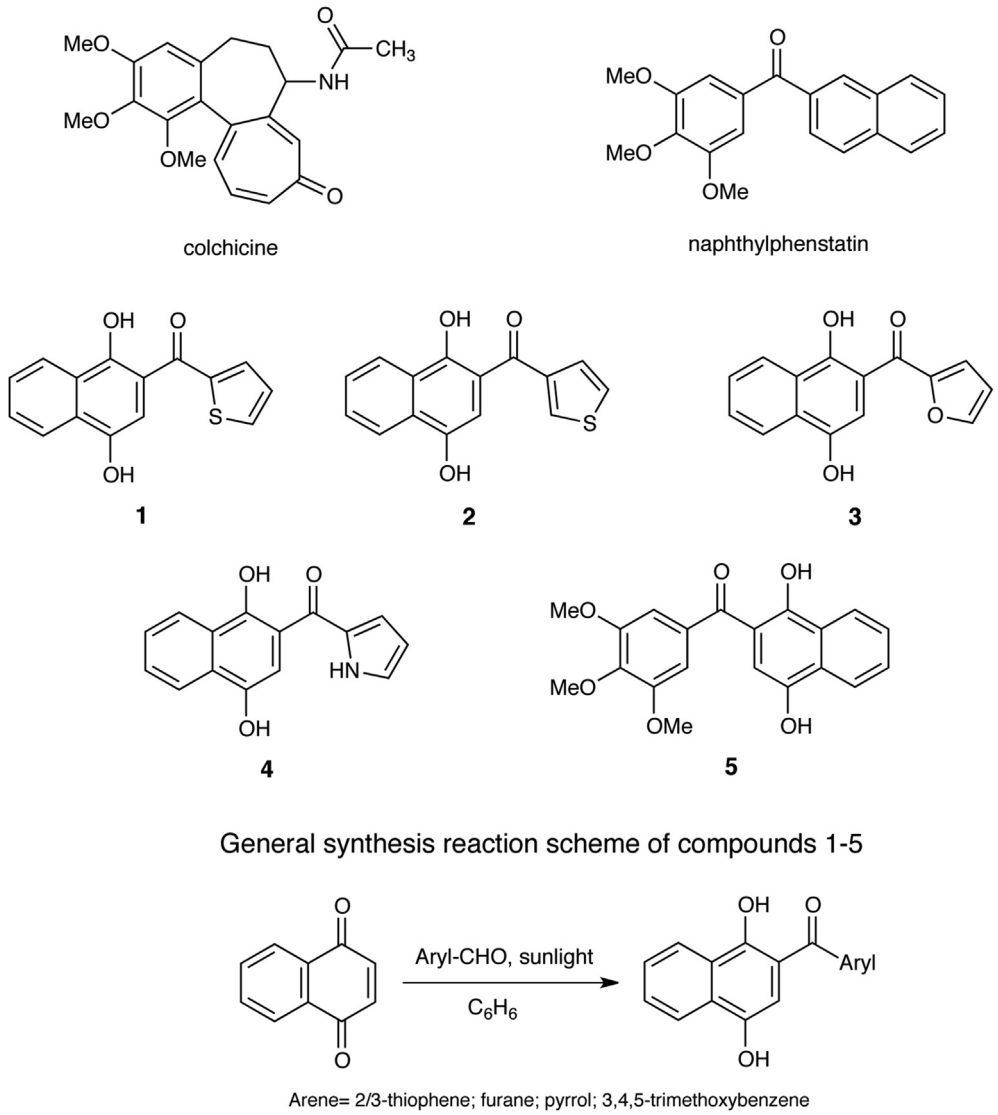


**Fig. 1.** Structure of colchicine, naphthylphenstatin and dNAKs **1**–**5** with their synthesis scheme.

### 2.2. dNAKs **1**–**5**

Compounds **1**–**4** were prepared from 1,4-naphthoquinone and the corresponding aldehydes: thiophene-2-carbaldehyde; thiophene-3-carbaldehyde; furan-2-carbaldehyde and 1*H*-pyrrole-2-carbaldehyde [17]. The structure of compounds **1**–**4** was confirmed by comparing the $^{1}H$, $^{13}C$ NMR spectral data to the data reported in the literature [18]. Compound **5** was prepared from 1,4-naphthoquinone and 3,4,5-trimethoxybenzaldehyde, and the spectral data were in agreement with those reported in the literature [20]. The dNAKs were purified by mean of flash chromatography on silica gel eluting with ethyl acetate/petroleum ether until no or trace impurity amounts (<1%) were detected by $^{1}H$ NMR at 400 MHz. Also, the purity of the dNAKs was checked by reverse phase HPLC chromatography at 220 nm showing purity for dNAKs **1**, **2**, **3**, **4** and **5** of 96, 96, 93, 98 and 95% respectively.

### 2.3. Partition coefficient assay

Octanol-water partition coefficient (LogP) values were determined for all compounds as described in Ref. [21].

### 2.4. Tubulin purification

Chicken brains were dissected from freshly slaughtered chickens (kindly donated by the Industrial Ochagavía Ltda, Ariztía, Santiago, Chile), kept on ice and used within 2 h. Tubulin was purified following the method described by Weisenberg et al. [22] with some modifications [23]. The stock protein was stored at −80 °C in the presence of 1 M sucrose. Tubulin concentration was determined by absorbance at 280 nm as described by Ortiz et al. [24]. Purity of tubulin was checked by SDS-gel electrophoresis. After the electrophoresis the gels were dried, and a digital image was acquired using a Sony camera (12.1 megapixels) with a 4× optical zoom. The images were analyzed with the Image J program.

### 2.5. Tubulin polymerization assay

To eliminate aggregates and equilibrate the polymerization buffer, the frozen tubulin sample was defrosted and filtered through a Sephacryl S-300 column, equilibrated with polymerization buffer. Once the tubulin concentration was determined, the samples were used for the assay. Tubulin polymerization was measured in a system allowing tubulin polymerization and depolymerization by changing the temperature. A quartz chamber was connected to two water baths at 4 °C and 37 °C, respectively. Absorbance at 350 nm was recorded at 4 °C for a short time (30 s), and this value was used as the baseline. Then, the temperature was increased to 37 °C. An exponential increase in absorbance reached a plateau due to the formation of microtubules. By decreasing the temperature to 4 °C, there was a sharp downturn in absorbance due to microtubule depolymerization. The polymerization buffer contained the following: 10 mM sodium phosphate pH 7.0, GTP (0.1 mM), $MgCl_2$ (16 mM), EGTA (1 mM) and 25% glycerol v/v.

### 2.6. Tubulin-colchicine binding inhibition

To measure the inhibition of the binding of colchicine to tubulin, the kinetics of colchicine fluorescence quenching, excited at 360 nm, was measured at 430 nm. The reaction mixture contained the following: phosphate buffer (20 mM, pH 7), tubulin (5 μM) and different concentrations of colchicine. Different concentrations of the compounds were added to the mixture and incubated for 10 min at 30 °C prior to the addition of colchicine. The fluorescence measurements were taken immediately after the addition of colchicine for the next 10 min.

The conformational change in tubulin induced by colchicine is responsible for the increment in the quantum yield of colchicine fluorescence [25]. This change is described by the following equation:

$$T + C \underset{}{\overset{K_c}{\rightleftarrows}} TC \underset{k_{-2}}{\overset{k_2}{\rightleftarrows}} T'C \quad (1)$$

where T is tubulin, T′ is tubulin in a different conformation, C is colchicine, $K_c$ is the colchicine binding constant, $k_2$ is the rate of tubulin conformational change and $k_{-2}$ is a very small conformational change reverse rate constant. The concentrations of colchicine were determined using the absorption coefficient ($E^{mM} = 16.6$ (350 nm)) provided by Sigma. The concentrations of compounds **3**, **4** and **5** were determined at 440, 421 and 420 nm in DMSO using the absorption coefficients 5,184, 8,829, and 5496 $M^{-1}cm^{-1}$, respectively.

### 2.7. Molecular docking

The Autodock Vina software [26] was used on a four-core Intel-processor machine. The crystallographic structure of tubulin deposited in the PDB database (1SA0) was used as the receptor [12]. This four-subunit structure (α2β2) was cleaved into two subunits (αβ), maintaining two MgGTP molecules in their respective sites. The colchicine molecule present in the structure was removed, and its binding site was used to dock the inhibitor molecules. The inhibitor molecules (ligands) were constructed and geometrically optimized using the Gaussian package software (Gaussian 03, Revision C.01, Gaussian, Inc.: 2003). For control purposes, we performed a search of the binding sites via conformational sampling on the protein surface with the ICM program and the Pocked Finder module [27]. The binding site was defined by a grid box of 20 Å × 20 Å × 15 Å around the colchicine binding site, and both the lateral chains of the binding site and the ligands were allowed to be flexible. The docking procedure resulted in ten different conformations (poses) of each ligand in the binding site, scored with a calculated ΔG°. Each pose was further analyzed, discarding the poses in which the ligand appeared to be outside the site. Further optimization of the binding sites was performed based on the molecular dynamics of the tubulin heterodimer to obtain different conformations, which were used for molecular docking. The docking free energy for the binding of each compound to each tubulin conformation was used to select the best site. This procedure was repeated for the binding site of Taxol, obtaining lower values of free energy (at least one order of magnitude lower) than those of colchicine in all cases.

The hydrogen bonds between the compounds and the amino acid residues of the binding site were determined and visualized using the computer program, LIGPLOT 2.10 [28].

## 3. Results

### 3.1. Effect of dNAKs on tubulin polymerization

Fig. 2A demonstrates the effects of dNAKs **1**–**5** (at different concentrations) on tubulin polymerization. All of the compounds decreased tubulin polymerization in a dose-dependent manner. Note that after cooling, turbidity decreased reaching mostly the initial values, indicating that polymerization of microtubules was reversible and almost not affected by the compounds. Compound **4** displayed the greatest tubulin polymerization inhibition, and the

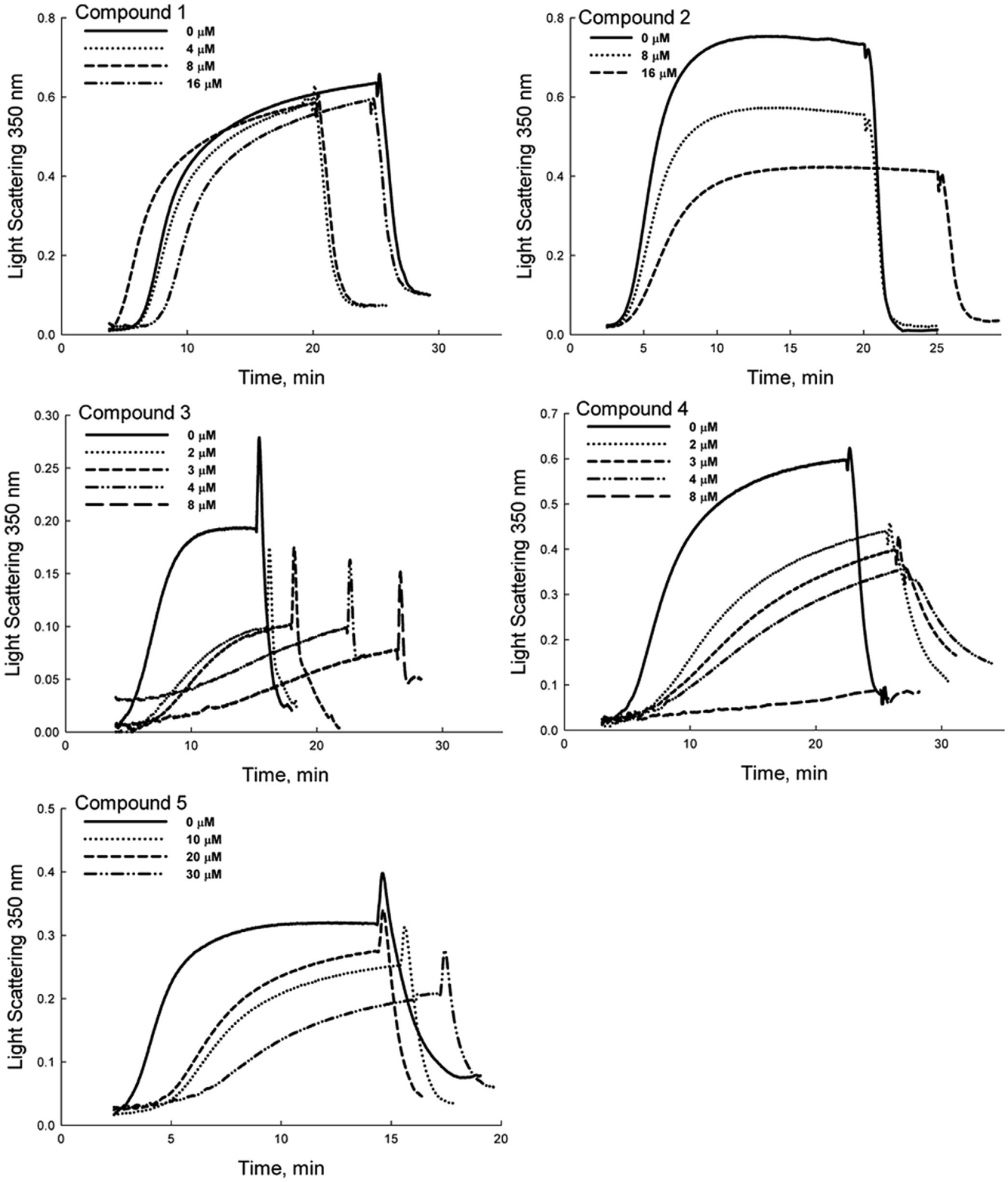


**Fig. 2. Inhibition of tubulin polymerization kinetics by the dNAKs**. Polymerization of 13.6 μM tubulin was followed by a change in turbidity at 350 nm, increasing the temperature to 37 °C at time zero. Depolymerization was induced by lowering the temperature to 4 °C, as indicated in the figures by a jump of turbidity, followed by fast diminution. The name and compound concentration are indicated in the figure.

least active compound was **1**. Table 1 shows the $IC_{50}$ values for each compound, as determined from their corresponding percent tubulin polymerization inhibition. Compound **4** inhibited the tubulin polymerization process to the greatest extent ($IC_{50} = 2.1$ μM). The least active compound was **1** ($IC_{50} = 170.4$ μM).

A further evaluation of the results from these inhibition assays indicated that compound **2** produced a stronger inhibitory effect on tubulin polymerization than did its positional isomer **1**, suggesting a remarkable geometrical preference of tubulin for ligand **2** compared to isomer **1**.

**Table 1**
Inhibition of tubulin polymerization (ITP), dissociation constant and LogP for dNAKs **1**–**5**.

| Structure | N° | ITP[a] | $K_{dis} \times 10^{6}$[b] | LogP[c] |
|---|---|---|---|---|
| 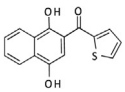 | **1** | 170.4 | nd[d] | 3.85 ± 0.41 |
| 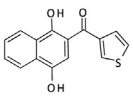 | **2** | 21.0 | nd[d] | 3.93 ± 0.80 |
| 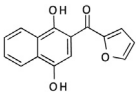 | **3** | 5.2 | 4.09 ± 0.86 | 3.04 ± 0.41 |
| 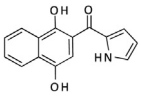 | **4** | 2.1 | 1.02 ± 0.23 | 2.41 ± 0.44 |
| 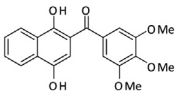 | **5** | 34.7 | 49.6 ± 12.3 | 4.33 ± 0.43 |

[a] ITP is expressed as $IC_{50}$ (μM).
[b] Determined by thermophoresis (Fig. S2).
[c] Determined experimentally, as described in the Experimental section. The SD corresponds to the mean of at least three experiments. nd, non-determined.
[d] The binding isotherm determined by thermophoresis was not analyzed because of saturation was not reached.

Due to the higher affinity of compound **4** for tubulin and the presence of colchicine trimethoxyphenyl ring in compound **5**, these were chosen to analyze its effect on the morphology of microtubules. Fig. S1 shows photographs obtained by transmission electron microscopy (20,000×) corresponding to microtubules under control conditions (1% DMSO) and tubulin sheets treated with compound **4** (4 μM) and compound **5** (17 μM). These results indicate that both compounds induced sheets of protofilaments, which is indicative of the inhibition of microtubule closure and may explain the decrease in the value of the slope of the straight lines used to calculate the critical concentrations (not shown). The widths of the microtubules and sheets were 24.52 ± 1.88 nm and 80.85 ± 31.11 nm, respectively.

### 3.2. Binding of dNAKs to tubulin

Fig. S2 illustrates the isotherm curves for the binding of these compounds to tubulin heterodimer. To work with the heterodimer, aggregates were eliminated by filtration chromatography in Sephacryl S-300, and the protein was used at nanomolar concentrations. The titration indicates that saturation was reached with each compound except **1** and **2** (not shown)**.** These experimental conditions allowed us to obtain very accurate dissociation constants. All values are in the low micromolar range, the smallest of which is observed for compound **4** ($K_{diss}$ = 1.02 ± 0.23 μM). This value is close to that of colchicine ($K_{diss}$ = 0.57 μM) reported as an average for neuronal β-tubulin [29], which is commonly used as a reference drug.

### 3.3. Tubulin colchicine binding inhibition

For the colchicine competitive experiments compounds **3**, **4** were chosen due to their higher tubulin affinity and solubility in aqueous buffer compared to the other compounds (Table 1), and compound **5** for the reason explained before. Fig. 3 demonstrates the inhibition of binding between colchicine and tubulin by compounds **3**, **4** and **5.** The intersection of the lines in the second quadrant in the Dixon plot and the parallel lines in the Cornish-Bowden plot [30] clearly demonstrate that the inhibition is competitive between these compounds and colchicine, suggesting that they share the same binding site. The values of the dissociation constants of the compounds ($K_d$) were obtained from the intercept with the abscissa in the second quadrant, according to the following relationship: $-[\text{compound}] = K_d(1+[\text{colchicine}]/K_c])$; the $K_c$ value for chicken brain tubulin was set to 0.7 μM experimentally determined by us. The inhibition constant values for compounds **3**, **4** and **5** were 2.7 ± 0.7 μM, 2.2 ± 0.9 μM and 2.6 ± 0.7 μM respectively.

### 3.4. Molecular docking and molecular dynamics of dNAKs bound to tubulin

The binding site and interactions of the dNAKs with tubulin were modeled using bioinformatics tools. As shown in Fig. 4, the best binding site for the compounds was located between both monomers of the heterodimer, resembling the binding site reported for colchicine and podophyllotoxin [12]. This binding site is located in a hydrophobic groove between helix H8 and strands S7–S8 of β-tubulin (Fig. 4A), whereas the polar ring of compounds **3** and **4** are pointing to the α-tubulin, in the heterodimer interface (Fig. 4B–C), the corresponding hydrophobic ring in compound **5** points in reverse direction (Fig. 4D). Other possible binding site studied was the taxol-binding site, but our analysis reveals that this has an insignificant affinity for the dNAKs.

All dNAKs bind to the same locus, but compounds **3**, **4** and **5**, have more contacts points with the protein molecule, remarking a better interaction. Compound **4** binds to the protein slightly overlapping the colchicine-binding site (Fig. 4C). The naphtyl ring is located at the aforementioned hydrophobic groove, but more displaced to the helix H8 of β-tubulin, where the lateral chains of Lys252 and Leu253 form a hydrophobic surface (Fig. 4C). Both residues also participate in the binding of colchicine. But the hydrophobic residues at the strands S7 and S8 do not play a role in the interaction of compounds **3** and **4** in contrast with colchicine. The polar pyrrole ring of compound **4** points to α-tubulin, at 3.5 Å from the hydroxyl group of Tyr224, existing the possibility of a hydrogen bond formation, but it is not completely clear from our simulation. The amide group of Asn101 in α-tubulin, between S5 and H5, forms one hydrogen bond with compound 3 and two hydrogen bonds with compound **4**, one with the hydroxyl group at C-1 and another with the oxygen of the bridge carbonyl group. The hydroxyl group at C-4 of both compounds forms two hydrogen bonds, one with the main chain nitrogen of Ala248 in β-tubulin and another with the oxygen of the amide group of Asn247 in β-tubulin (Fig. 4B–C). The nitrogen of the amide group of Asn256 in β-tubulin could form a hydrogen bond hydroxyl group at C-1 of naphtyl group of these compounds; however, in our simulation, the distance between these groups is 3.8 Å. Compound **5** binds to the same colchicine-binding site, in inverse direction but with a higher degree of overlapping (Fig. 4D). The 3,4,5-trimethoxyphenyl moiety locates in the same hydrophobic pocket that of colchicine A-ring, between the helix H8 and strands S7–S8 of β-tubulin. The hydroxyl group at C-4 in compound **5**, kept the same two hydrogen bonds with the amide group of Asn247 and Ala248 as with compound **4** and the interaction of the hydroxyl group at C-1 is missing (Fig. 4D). No polar contacts of compound **5** with residues of α-tubulin were observed. These interactions explain the lower affinity of compound **5** respects to compound **3** and **4** for tubulin. Compounds **1** and **2** bind like compound **4** with similar interactions but they were not further analyzed.

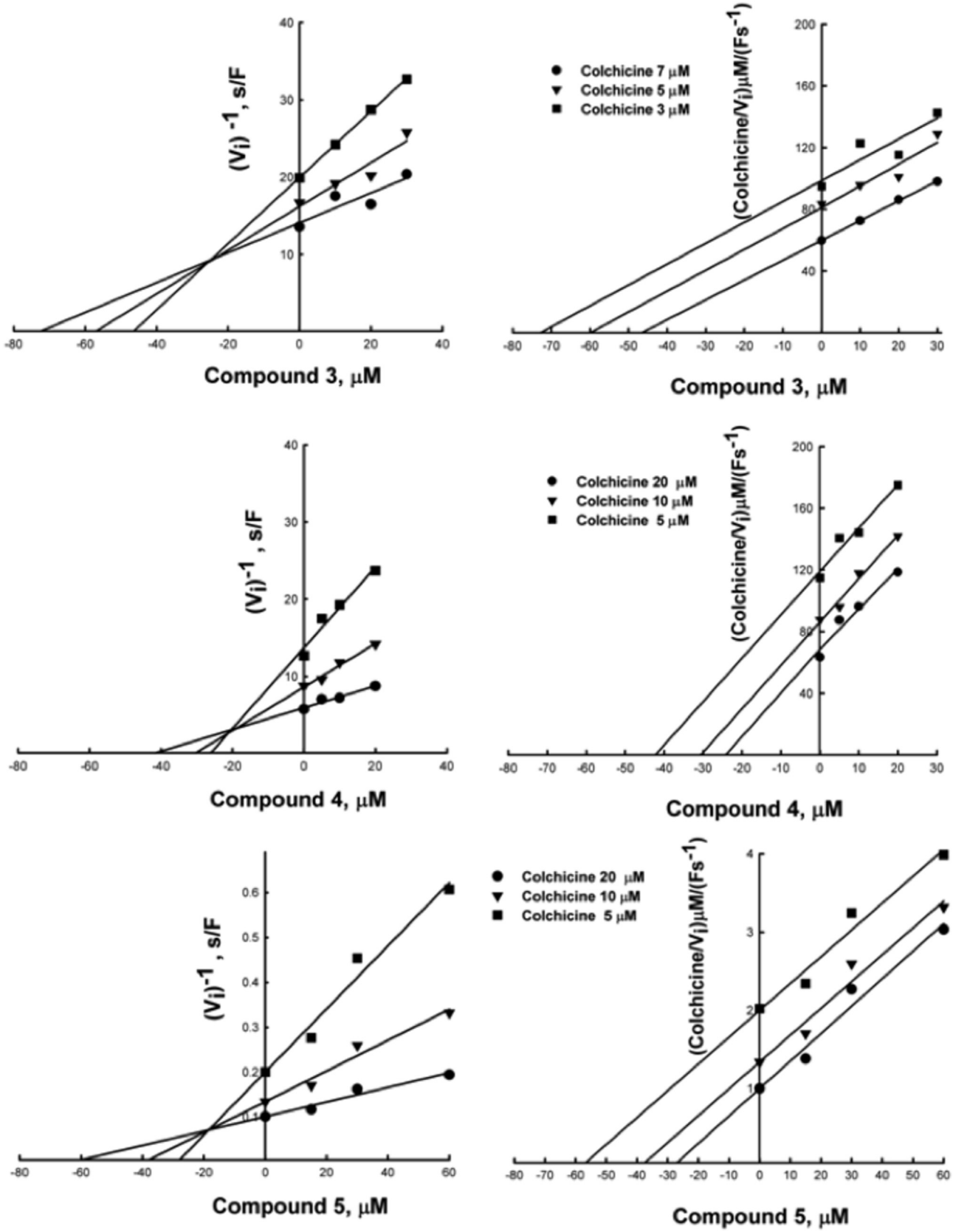


**Fig. 3. Dixon (left) and Cornish-Bowden (right) plots for the inhibition of tubulin-colchicine complex formation by dNAKs 3, 4 and 5**. The initial velocity values for the formation of the fluorescent tubulin-colchicine complex were measured following the increment of fluorescence at 430 nm using an excitation wavelength of 360 nm. The experimental conditions are described in Material and methods. The concentrations of colchicine are indicated in the figure.

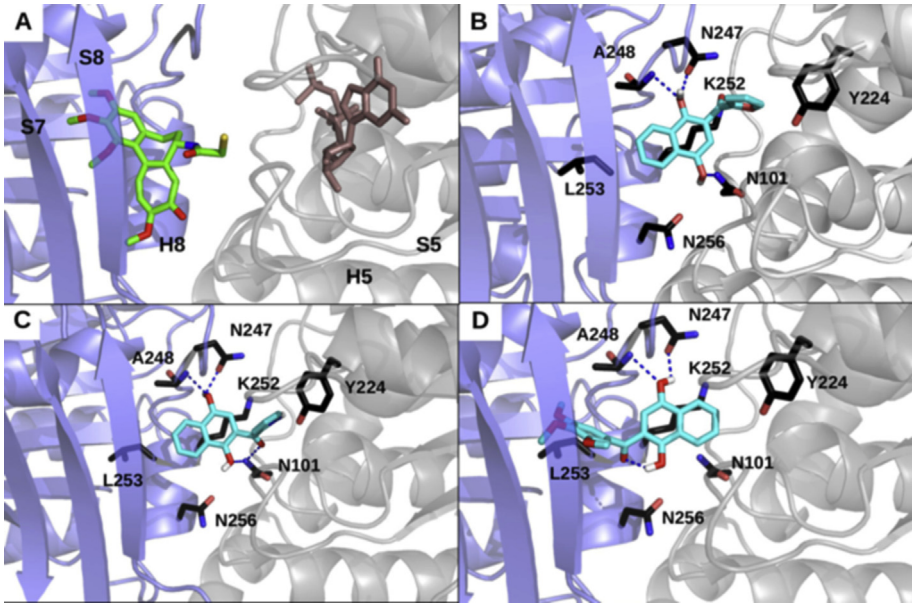


**Fig. 4. Binding site model of dNAKs 3, 4 and 5 in αβ-tubulin heterodimer.** A. αβ-tubulin taken from the 1SA0 PDB file showing the structure around the colchicine-binding site region (green stick) and GTP in its binding site in α-tubulin (brown stick). The number of secondary structure elements are indicated β-tubulin (blue) and in α-tubulin (gray). B. Docking of compound **3** in the absence of colchicine with αβ-tubulin heterodimer. The secondary structure is the same as in A. Compound **3** is cyan in stick representation, and it is bound in a position that partially overlaps the colchicine-binding site. GTP was omitted for clarity. C and D. Same as in B but with compounds **4** and **5** respectively. Amino acid residues involved in the interaction of compounds **3**, **4** and **5** with αβ-tubulin are labeled with their respective sequence number and dashed lines indicate hydrogen bonds.

## 4. Discussion

The dNAKs exhibit tubulin polymerization inhibitory activity, with $IC_{50}$ values ranging from 2.1 to 174 μM, and the $IC_{50}$ values for compounds **3**, **4** and **5** are coincident with their dissociation constants, as determined by thermophoresis. Among the members of this series, compound **4**, which contain the pyrrol-2-yl substituent, displayed higher affinity and inhibitory activity, whereas the activity of compound **1**, which contains a 2-thienyl substituent, was lower. Compound **2** displayed an eight-fold potency increase compared to the corresponding position in isomer **1**, which could be attributed to more favorable binding between tubulin and the 3-thienyl fragment of the former ligand compared to the thien-2-yl fragment of the latter. The replacement of the trimethoxyphenyl group of compound **5** by fur-2-yl-, thien-3-yl- and pyrrol-2-yl fragment in **3**, **2** and **4**, respectively, enhanced the polymerization inhibitory activity in the following order: **4** > **3** >> **2**.

To locate the tubulin-binding site for dNAKs **3**, **4** and **5** colchicine binding inhibition experiments were done (Fig. 3). The inhibition constant values for compounds **3** and **4** were similar than those obtained from microtubule polymerization and thermophoresis, and six time lower for compound 5 which has the structure most similar to colchicine. The only reasonable explanation for this discrepancy is that the affinity of colchicine for tubulin increases with incubation time, reaching nanomolar values for $K_c$ after one hour [31] due to the conformational change of tubulin induced by colchicine [25]. From Equation (1) the simplest equilibrium among colchicine and its derivative compounds with tubulin is given by:

$$\begin{array}{ccc} & \overset{K_c}{} & \overset{k_2}{} \\ T + C & \rightleftarrows TC & \rightleftarrows T'C \\ D \downarrow\uparrow K_d & & \overset{}{k_{-2}} \\ TD & & \end{array} \qquad (2)$$

where T is tubulin, T′ is a different conformation, C is colchicine, D is the dNAK **3, 4** or **5**, $K_c$ and $K_d$ are the colchicine and dNAK dissociation constants, respectively, $k_2$ is the rate for tubulin conformational change and $k_{-2}$ is a very small conformational change backward rate constant.

Therefore, to correct for the effect of time on the affinity of tubulin for colchicine, we calculated the dissociation constant of the tubulin-colchicine complex ($K_c$) using the experimental values of the dissociation constants of compounds **3**, **4** and **5** and the values of the intersection with the abscissa in the second quadrant obtained from the Dixon plots (Fig. 3). The $K_c$ values calculated using the thermophoresis $K_d$ values of both compounds (Table 1) provided an average value of 0.31 ± 0.1 μM for the binding of colchicine to chicken brain tubulin, value that is in the same micromolar range of the dissociation constant (0.7 μM) that we determined experimentally for the complex colchicine-tubulin.

The binding of dNAKs **3**, **4** and **5** to tubulin colchicine binding site was confirmed by molecular docking and molecular dynamics, showing that the binding site of these compounds is located in the same region of colchicine binding site at the interface of the α and β tubulin in the heterodimer. It is important to remember that most depolymerizing microtubule compounds bind to the vinblastine- or colchicine-binding site in tubulin [4,32]. Hence, the dNAKs act in a similar manner because they inhibit microtubule assembly and colchicine binding to the tubulin heterodimer. In fact, dNAKs are competitive inhibitors of colchicine binding to tubulin, and they share a portion of the colchicine-binding site.

## Acknowledgments

We thank the Fondo Nacional de Ciencia y Tecnología (Grants N° 1100376 and 1130711) and the Commission of the European Communities SFP 223431 for providing financial support for this study. We thank the Nanotemper technology GmbH for allowing us to use the instrument Monolith, NT 115. We also thank the following for their assistance: L. Pouchucq for electron microscopy experiments, B. Poblete for bioinformatics analysis, G. Araya and M. Espinosa for physicochemical characterization of the compounds.

## Appendix A. Supplementary data

Supplementary data related to this article can be found at http://dx.doi.org/10.1016/j.bbrc.2015.09.041.

## Transparency document

Transparency document related to this article can be found online at http://dx.doi.org/10.1016/j.bbrc.2015.09.041.

## References


[1] E. Nogales, Structural insight into microtubule function, Annu. Rev. Biophys. Biomol. Struct. 30 (2001) 397–420.
[2] H.P. Erickson, E.T. O'Brien, Microtubule dynamic instability and GTP hydrolysis, Annu. Rev. Biophys. Biomol. Struct. 21 (1992) 145–166.
[3] J. Zhou, P. Giannakakou, Targeting microtubules for cancer chemotherapy, Curr. Med. Chem. Anti-Cancer Agents 5 (2005) 65–71.
[4] M.A. Jordan, L. Wilson, Microtubules as a target for anticancer drugs, Nat. Rev. Cancer 4 (2004) 253–265.
[5] S. Lobert, B. Vulevic, J.J. Correia, Interaction of vinca alkaloids with tubulin: a comparison of vinblastine, vincristine, and vinorelbine, Biochemistry 35 (1996) 6806–6814.
[6] K.H. Altmann, M. Wartmann, T. O'Reilly, Epothilones and related structures – a new class of microtubule inhibitors with potent in vivo antitumor activity, Biochim. Biophys. Acta 1470 (2000) 79–91.
[7] K. Kamath, M.A. Jordan, Suppression of microtubule dynamics by epothilone B is associated with mitotic arrest, Cancer Res. 63 (2003) 6026–6031.
[8] J.H. Nettles, H. Li, B. Cornett, J.M. Krahn, et al., The binding mode of epothilone A on α,β-tubulin by electron crystallography, Science 305 (2004) 866–869.
[9] S.B. Hastie, Interactions of colchicine with tubulin, Pharmacol. Ther. 51 (1991) 377–401.
[10] D. Panda, J.E. Daijo, M.A. Jordan, L. Wilson, Kinetic stabilization of microtubule dynamics at steady state in vitro by substoichiometric concentrations of tubulin-colchicine complex, Biochemistry 34 (1995) 9921–9929.
[11] L. Wilson, D. Panda, M.A. Jordan, Modulation of microtubule dynamics by drugs: a paradigm for the actions of cellular regulators, Cell Struct. Funct. 29 (1999) 329–335.
[12] R.B. Ravelli, B. Gigant, P.A. Curmi, et al., Insight into tubulin regulation from a complex with colchicine and a stathmin-like domain, Nature 428 (2004) 198–202.
[13] U. Lange, Current aspects of colchicine therapy: classical indications and new therapeutic uses, in: F.H. Columbus (Ed.), Arthritis Research: Treatment and Management, Nova Sci. Publishers Inc, 2005. Chap III.
[14] O.N. Zefirova, A.G. Diikov, N.V. Zyk, N.S. Zefirov, Ligands of the colchicine site of tubulin: a common pharmacophore and new structural classes, Russ. Chem. Bull. Int. Ed. 56 (2007) 680–688.
[15] B. Bhattacharyya, D. Panda, S. Gupta, M. Banerjee, Anti-Mitotic activity of colchicine and the structural basis for its interaction with tubulin, Med. Res. Rev. 28 (2008) 155–183.
[16] A.S. Negi, Y. Gautam, S. Alam, et al., Natural antitubulin agents; Importance of 3,4,5-trimethoxyphenyl fragment, Biorg. Med. Chem. 23 (2015) 373–389.
[17] J. Benites, D. Ríos, P. Díaz, J.A. Valderrama, The solar–chemical Photo-Friedel-Crafts heteroacylation of 1,4-quinones, Tetrahedron Lett. 52 (2011) 609–611.
[18] P. Arenas, A. Peña, D. Ríos, et al., Eco-friendly synthesis and antiproliferative evaluation of oxygen substituted diaryl ketones, Molecules 18 (2013) 9818–9832.
[19] C. Álvarez, R. Alvarez, P. Corchete, Naphthylphenstatins as tubulin ligands: synthesis and biological evaluation, Bioorg. Med. Chem. 16 (2008) 8999–9008.
[20] J. Iribarra, D. Vásquez, C. Theoduloz, et al., Synthesis and antitumor evaluation of 6-arylsubstituted benzo[j]phenanthridine- and benzo[g]pyrimido[4,5-c] isoquinolinequinones, Molecules 17 (2012) 11616–11629.
[21] J. Benites, E. Gutiérrez, J. López, et al., Evaluation of analgesic activities of tremetone derivatives isolated from the Chilean Altiplano medicine *Parastrephia lepidophylla*, Nat. Prod. Commun. 7 (2012) 611–614.
[22] R.C. Weisenberg, G.G. Borisy, E.W. Taylor, The colchicine-binding protein of mammalian brain and its relation to microtubules, Biochemistry 7 (1968) 4466–4479.
[23] O. Monasterio, S.N. Timasheff, Inhibition of tubulin self-assembly and tubulin-colchicine GTPase activity by guanosine5'-(γ-fluorotriphosphate), Biochemistry 26 (1987) 6091–6099.
[24] M. Ortiz, R. Lagos, O. Monasterio, Interaction between the C-terminal peptides of tubulin and tubulin S detected with the fluorescence probe 4'-6-diamidino-2-phenylindole, Arch. Biochem. Biophys. 303 (1993) 159–164.
[25] A. Lambeirt, Y.A. Engelborghs, A Fluorescence stopped flow study of colchicine binding to tubulin, J. Biol. Chem. 256 (1981) 3279–3282.
[26] O. Trott, A.J. Olson, AutoDock Vina: improving the speed and accuracy of docking with a new scoring function, efficient optimization, and multithreading, J. Comput. Chem. 31 (2010) 455–461.
[27] J. An, M. Totrov, R. Abagyan, Pocketome via comprehensive identification and classification of ligand binding envelopes, Mol. Cell Proteomics 4 (2005) 752–761.
[28] A.C. Wallace, R.A. Laskowski, J.M. Thornton, LIGPLOT: a program to generate schematic diagrams of protein-ligand interaction, Protein Eng. 8 (1995) 127–134.
[29] R.G. Burns, Analysis of the colchicine-binding site of β-tubulin, FEBS Lett. 297 (1992) 205–208.
[30] A.A. Cornish-Bowden, Simple graphical method for determining the inhibition constants of mixed, uncompetitive and noncompetitive inhibitors, Biochem. J. 137 (1974) 143–144.
[31] J.F. Diaz, J.M. Andreu, Kinetics of dissociation of the tubulin-colchicine complex, J. Biol. Chem. 266 (1991) 2890–2896.
[32] L. Wilson, I. Meza, The mechanism of action of colchicine. Colchicine binding properties of Sea Urchin sperm tail outer doublet tubulin, J. Cell. Biol. 58 (1973) 709–719.